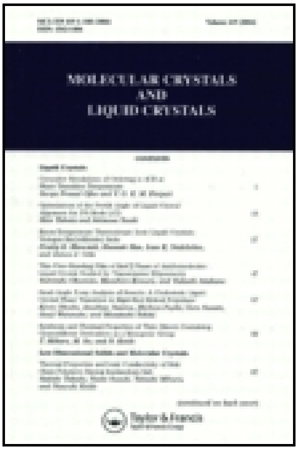

Molecular Crystals and Liquid Crystals
Publication details, including instructions for authors and subscription information:
http://www.tandfonline.com/loi/gmcl20

Crystallization Kinetics Study on Tilted Ordering in N-(p-n-Alkoxybenzylidene)-p-n-Alkylanilines (nO·m Compounds) by Thermal and Electrical Techniques Part II

T. Chitravel [a], M. L. N. Madhu Mohan [b] & V. Krishnakumar [c]

[a] Department of Physical Sciences, Bannari Amman Institute of Technology, Sathyamangalam, India

[b] Liquid Crystal Research Laboratory, Bannari Amman Institute of Technology, Sathyamangalam, India

[c] Department of Physics, Periyar University, Salem, India

Version of record first published: 31 Aug 2012.

To cite this article: T. Chitravel , M. L. N. Madhu Mohan & V. Krishnakumar (2008): Crystallization Kinetics Study on Tilted Ordering in N-(p-n-Alkoxybenzylidene)-p-n-Alkylanilines (nO·m Compounds) by Thermal and Electrical Techniques Part II, Molecular Crystals and Liquid Crystals, 493:1, 17-30

To link to this article: http://dx.doi.org/10.1080/15421400802406422

Mol. Cryst. Liq. Cryst., Vol. 493, pp. 17–30, 2008
Copyright © Taylor & Francis Group, LLC
ISSN: 1542-1406 print/1563-5287 online
DOI: 10.1080/15421400802406422

Crystallization Kinetics Study on Tilted Ordering in N-(p-n-Alkoxybenzylidene)-p-n-Alkylanilines (nO·m Compounds) by Thermal and Electrical Techniques Part II

T. Chitravel[1], **M. L. N. Madhu Mohan**[2], **and**
V. Krishnakumar[3]
[1]Department of Physical Sciences, Bannari Amman Institute of Technology, Sathyamangalam, India
[2]Liquid Crystal Research Laboratory, Bannari Amman Institute of Technology, Sathyamangalam, India
[3]Department of Physics, Periyar University, Salem, India

A systematic kinetic study of crystallization among two smectogens of higher homologues of the benzylideneaniline nO·m series viz *15O.8 and 15O.10 has been carried out by thermal microscopy, differential scanning calorimetry (DSC), and dielectric studies. The crystallization kinetics was studied by two techniques* viz *the traditional thermal analysis (DSC) and electrical studies* viz *capacitance and dielectric loss variation with temperature. The DSC thermograms were run from crystallization temperature to the isotropic melt for different time intervals. The liquid crystalline behavior together with the rate of crystallization of smectic ordering in newly synthesized nO·m compounds were discussed in relation to the kinetophase (which occurs prior to the crystallization). The molecular mechanism and dimensionality in the crystal growth were computed from the Avrami equation. The characteristic crystallization time (t^*) at each crystallization temperature was deduced from the individual plots of $\log t$ and ΔH. Further, it was observed that the data obtained from DSC and dielectric studies were in good agreement with one another.*

Keywords: crystallization kinetics; dielectric study; DSC; nO · m compounds

1. INTRODUCTION

The smectic orderings exhibited by liquid crystals can be broadly classified as orthogonal and tilted phases. The molecules in the orthogonal smectic phases are parallel to each other with their long axes

Address correspondence to V. Krishnakumar, Department of Physics, Periyar University, Salem 636011, India. E-Mail: vkrishna_kumar@yahoo.com

perpendicular to the layer plane, resulting in free rotation of the molecules around the long molecular axis [1]. Consequently, in the case of tilted phase, the significant difference is the tilt of the molecular long axes with respect to the layer normal, leading to the hindered rotation of the molecule along the long axis. Furthermore, the layer thickness in a tilted mesophase is smaller than the molecular length, while in the case of orthogonal ordering they are approximately equal. This degree of variation in the layer thickness, coupled with the molecular rotation, has a significant influence on the rate of crystallization. In fact, the distribution of heat transformation in both orderings, which has a direct impact on the rate of crystallization, is rather a complicated process, which may be elucidated structurally by detailed X-ray investigation. Alternatively, the study of crystallization kinetics [2,3] is a powerful tool to understand the various mechanisms involved in crystallization of liquid crystals.

The liquid crystalline materials belonging to the class of benzylideneaniline exhibit a fascinating mesomorphic behavior associated with a distinct molecular ordering; the convenient working thermal range makes them suitable for systematic kinetic investigations. In continuation of our experimental studies [4,5] on nO·m and ferroelectric liquid crystals, here we present a detailed analysis of two smectogens of higher homologues of the benzylideneaniline nO·m series *viz* 15O.8 and 15O.10.

2. EXPERIMENTAL

The nO·m compounds of the present investigation were synthesized and characterized as reported earlier [6]. The crystallization kinetics of the present compounds, determined by the rate of growth of a particular transition, were performed on a Shimadzu DSC-60 differential scanning calorimeter and Agilent 4192 A LF impedance analyzer. The thermograms at each crystallization temperature, together with simultaneous phase identification [7] were obtained using a Instec Standalone Temperature Controller (STC 200) supplemented by Nikon polarizing microscope. The DSC measurements were performed on each member of pure nO·m compounds (3–7 mg sample) using aluminum and/or glass crucibles. A typical DSC scan for a given sample at each crystallization temperature is described as follows. The sample was heated to its isotropic melt with a scan rate of 10°C min^{-1}; after holding for 1 minute to attain thermal equilibrium, the sample was cooled at the same scan rate to its predetermined crystallization temperature. After holding for a requisite time interval at crystallization temperature, the endothermic peaks were recorded while the sample was cooled to the crystal state at of 10°C min^{-1}. This process was repeated for each individual member of the nO·m series at the appropriate preselected crystallization temperatures.

For the elucidation of the dielectric data, the nO·m sample under investigation was filled in a 4 micron spacer polyamide buffed cells (Instec Inc. USA) in its isotropic state under vacuum. Silver paste and wires were used to draw the electrodes from the cell. The cell was placed in an Instec hot and cold stage (HCS402) equipped with Instec Standalone Temperature Controller (STC 200). The temperature is monitored and controlled through a computer by a software program to an accuracy of ±0.01°C. The sample was heated to its isotropic melt with a scan rate of 10°C min^{-1}; after holding for a period of 1 minute time to attain thermal equilibrium, the sample was cooled at the same scan rate to its predetermined crystallization temperature. After holding for a requisite time interval at crystallization temperature, the data of capacitance and dielectric loss were noted for each time interval. This process was repeated for each individual member of the nO·m series at the appropriate preselected crystallization temperatures.

2.1. Synthesis of the Compounds

The compounds were prepared [6,7] by condensation of the respective alkoxy benzaldehyde (0.1 mole) and alkyl aniline (0.1 mole) in refluxing in absolute ethanol in the presence of a few drops of glacial acetic acid. After refluxing the reactants for 4 hours, the solvent was removed by distillation under reduced pressure. The crude sample was subjected to repeated recrystallization from cold absolute ethanol, till transition temperatures were found to be reproducible.

The homologous series N-(p-n-alkoxybenzylidene)-p-alkylaniline are Schiff bases with the general molecular formula is given below:

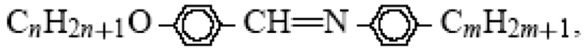

where n and m represents the number of carbon atoms in alkoxy and alkyl end chains, respectively. The anilines used for the synthesis of the above compounds are obtained from Sigma Aldrich Chemicals while the alkoxybenzaldehydes were prepared in our laboratory.

2.2. Synthesis of p-n-Pentadecyloxy Benzaldehyde

To a cyclohexanone solution containing p-hydroxybenzaldehyde (1.83 gm/15 mmol) and n-pentadecyl bromide (5.82 ml/20 mmol), 5.15 gm of (37.5 mmol) of anhydrous potassium carbonate was added slowly with constant stirring. The reaction mixture was then heated under reflux for 3 hours until the evolution of CO_2 ceased. After cooling to room temperature, the reaction mixture was filtered off to remove excess of K_2CO_3 and KBr formed during the reaction. The precipitate was washed repeatedly with excess of ether. On evaporation, the excess ether and cyclohexanone under reduced pressure, a colorless oil product (85% yield) was obtained. The oil product was further purified by passing through a silica gel column using a mixture of benzene and acetone in the volume ratio 1:4.

3. RESULT AND DISCUSSION

3.1. Phase Identification

The observed phase variants, transition temperatures, and corresponding enthalpy values obtained by thermal microscopy, dielectric studies, and DSC are presented in Table 1. The compounds of the present nO·m series are found to exhibit characteristic textures [8], *viz* broken focal-conic texture in smectic F phase. The smectic F phase with monoclinic symmetry [9], and long range tilt order, possessing a hexagonal molecular packing with in the smectic layers (normal to the long axis of the molecules), has a quasi 2-dimentional solid structure (*i.e.*, poor correlation between layers).

The 15O.8 and 15O.10 exhibits mono-variant phase sequence (Smectic F). Further the phase transition temperatures observed by thermal microscopy are found to be in good agreement with those obtained from DSC and dielectric studies (Table 1).

TABLE 1 Transition Temperatures (in °C) Obtained from TM, DSC, and Dielectric Studies of nO.m Compounds. Corresponding Enthalpy Values (in J/g) are Given in Parenthesis

				Dielectric studies			
				Capacitance		Dielectric loss	
nO.m	Phase transition	TM	DSC	10 KHz	100 KHz	10 KHz	100 KHz
15O.8	Isotropic–SmF	82.5	82.85 (14.97)	82.7	82.5	82.7	82.5
	Sm F–Crystal	40.9	40.03 (45.53)	42.1	41.5	42.3	41.5
15O.10	Isotropic–SmF	84.7	83.15 (35.09)	83.9	83.8	84.7	83.9
	Sm F–Crystal	44.3	41.00 (45.56)	44.9	44.7	44.3	44.5

3.2. Selection of Thermal Range of Crystallization Temperatures

The procedure for the thermal selectivity for the crystallization temperatures (CT) is described for 15O.8. The DSC thermograms of the 15O.8 is illustrated in Fig. 1. The compound 15O.8 is taken as a representative member of the present work, it exhibits two distinct transitions in the cooling run at 82.85°C and 40.03°C with heat of transition 14.97 J/g and 45.53 J/g, respectively. From this data it is inferred that the thermal span of mesomorphic phase as ($T_{Iso\text{-}SmF}$,)-($T_{SmF\text{-}Cry}$) is 42.82°C. Once the $T_{Iso\text{-}SmF}$ is completed the kinetics of crystallization from smectic F could be investigated over a temperature range between $T_{SmF\text{-}Cry}$. provided if the crystallization kinetics are not too fast.

3.3. Crystallization Kinetics Through DSC

The crystallization kinetics of 15O.8 relating to the phase transition from Smectic F to the melt is selectively performed at each predetermined crystallization temperatures *viz* 81, 71, 61, and 51°C, respectively. The sample is held at 81°C for different time intervals (0.1 to

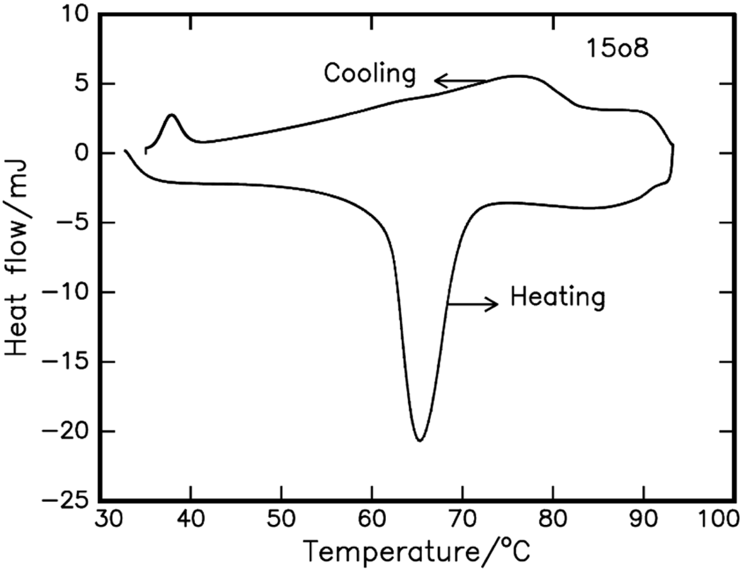

FIGURE 1 DSC heating and cooling thermograms of 15O.8 recorded at a scan rate of 10°C min^{-1}.

7 minutes). The heating curve with a crystallization time of t = 0 min is recorded immediately following the quenching of the crystal to melt, at crystallization temperature 81°C.

The enthalpy values for individual transitions at different time intervals are calculated at each crystallization temperature, and the corresponding data plotted against the corresponding logarithm of time intervals for each member of nO · m series. A plot of heats of melting of the mesomorphic phase, *viz* the log of annealing time for different crystallization temperatures of 15O.8, obtained by shifting data along the log t axis to the 61°C curve is depicted in Fig. 2. These plots have an identical shape, apart from the shift in the log t axis suggesting the limitations of the rate of crystallization kinetics [10]. Furthermore, simultaneous measurement of the heats of melting of the smectic F endotherm with time shows, without ambiguity, that the affective beginning and end of the crystal formation process coincides with those of the decay of smectic F phase, illustrating a direct smectic F to crystal phase conversion. Such a master curve strongly suggests that the same mechanism operates for crystallization from the smectic F to crystal for both the compounds. As expected [10], the overall crystallization rate is controlled by a nucleation rate influencing the rate

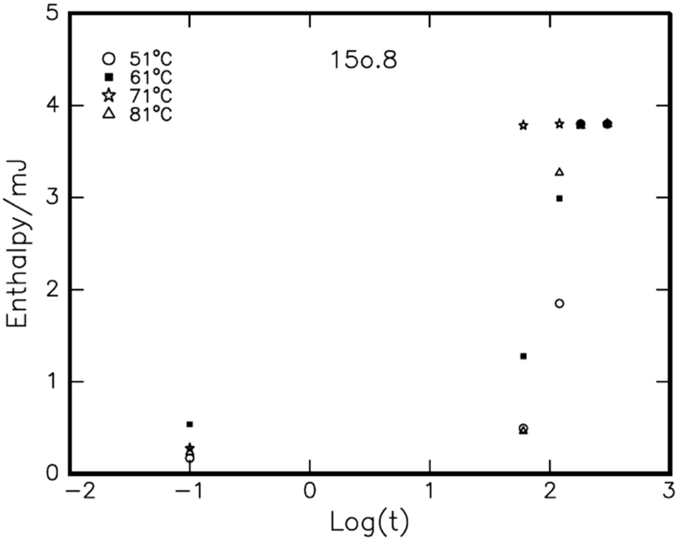

FIGURE 2 Plot of heats of melting of the mesomorphic phase of 15O.8 *viz* the log of the annealing time for different temperatures, obtained by shifting data along the log t axis to the 61°C.

of growth of domains; this is a function of the degree of super cooling and the starting smectic mesophase.

Similar experimental studies are carried out for measurement of crystallization kinetics of the other compound (15O.10) of this homologous series. The corresponding data of crystallization time t^* along with the calculated crystal growth parameters for different crystallization temperatures are summarized in Table 2, which includes the results relevant to the following sections.

3.4. Crystallization Kinetics Through Dielectric Studies

It was earlier proposed by us [5] that the crystallization kinetics can also be studied and analyzed at a selected frequency with the dielectric data. The crystallization kinetics relating to the phase transition from Smectic F to the melt of 15O.8 is selectively performed at each predetermined crystallization temperatures *viz* 51, 61, 71, and 81°C, respectively, at an excitation frequency of 1 KHz. The sample is held at 51°C for different time intervals (0.1 to 10 minutes). The dielectric data (capacitance and dielectric loss) at 1 KHz excitation frequency with a crystallization time of $t = 0$ to 10 min are recorded immediately following the quenching of the crystal to melt, at crystallization temperature 51°C. The capacitance and dielectric loss values for individual transitions at different time intervals are noted at each crystallization temperature, and the corresponding data plotted against the logarithm of time intervals for each member of $nO \cdot m$ series. The logarithm of the constant b obtained by dielectric studies (ε' and ε'') as a function of crystallization temperatures for the compound 15O.10 is depicted in Fig. 3. From Fig. 3 it can be inferred that the growth mechanism follows a uniform trend for all the temperature studied in the present compound. Crystallization obtained by this technique for 15O.10 compound at 45, 61, 71, and 81°C are identical to those of DSC data curves suggesting the existence of the same mechanism in the rate of crystallization kinetics [4].

3.5. The Process of Crystallization

In general, the kinetics of crystallization involving the rate of growth of small domains in a smectic phase is manifested equally by its temperature and time. Temperature dependence of nucleation, taking place as a homogeneous process over a constant period of time leads to the phenomenon of sporadic growth. In addition, defects and impurities in the compound have a pronounced influence on the nucleation process [10]. Further contributions from solid state transformations,

TABLE 2 Measured Crystallization Parameters for 63.2% Transformation from the Various Smectic Mesophases to the Crystalline Phase of nO.m Compounds Experimentally Obtained by Thermal Land Electrical Studies

		Thermal studies			Electrical studies					
					Dielectric studies (1 KHz)					
		Differential scanning calorimetry (ΔH)			Permittivity (ε')			Dielectric loss (ε'')		
nO.m	CT/°C	t*/sec	n	b	t*/sec	n	b	t*/sec	n	b
15O.8	81	103.03	1.478	0.105×10^{-2}	279.12	0.4523	0.783×10^{-1}	215.21	0.6716	0.2711×10^{-1}
	71	43.03	2.016	0.508×10^{-3}	254.10	0.4674	0.751×10^{-1}	139.10	0.5144	0.3191×10^{-1}
	61	103.90	2.3111	0.196×10^{-4}	270.0	0.4188	0.958×10^{-1}	239.13	0.5334	0.336×10^{-1}
	51	139.56	2.987	0.392×10^{-6}	328.68	0.5306	0.462×10^{-1}	509.58	0.5443	0.7897×10^{-1}
15O.10	81	41.25	0.786	0.5373×10^{-1}	274.45	0.3062	0.1796	201.07	0.3381	0.1664
	71	41.26	0.7839	0.5433×10^{-1}	721.67	0.2572	0.1840	205.42	0.2861	0.1879
	61	43.03	0.7781	0.588×10^{-1}	747.77	0.2650	0.2202	435.61	0.2060	0.1885
	45	97.39	0.6068	0.623×10^{-1}	135.0	0.2750	0.2595	170.42	0.3125	0.2207

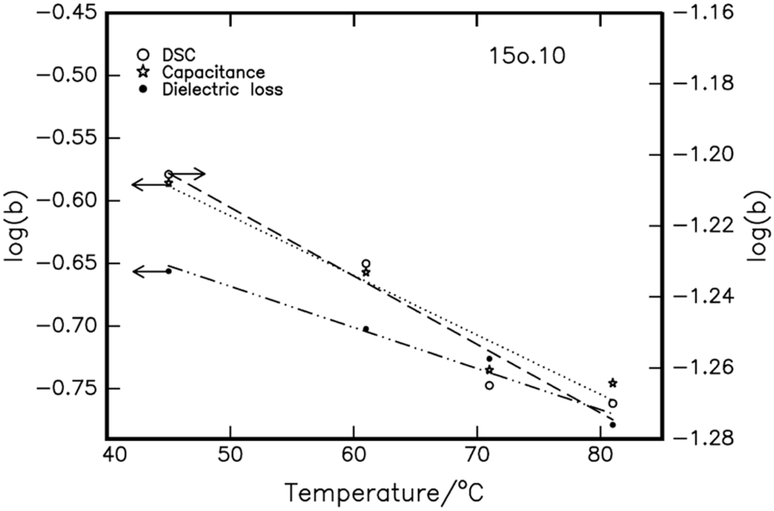

FIGURE 3 The logarithm of the constant b obtained by dielectric studies (ε' and ε'') as a function of crystallization temperatures for the compound 15O.10.

where growth occurs only at the surface of the nuclei, hampers the overall rate of phase transformation and the dimensional geometry of the growing domains.

It is well known that the crystallization process involving the fraction of the transformed volume x, at a time t measured since the beginning of the crystallization process, is described by the Avrami equation [2,3]

$$x = 1 - \exp(-bt^n), \tag{1}$$

where the constant b and n depend on the nucleation mechanism and the dimensionality geometry of the growing domains, respectively. The transformed volume x at a crystallization time t is given by $\Delta H/\Delta H_o$ where ΔH is the crystal heat of melt measured at time t and ΔH_o is the maximum value obtained from the plateau of the individual master curves (Fig. 3). A similar argument holds good for dielectric data $\Delta\varepsilon'/\Delta\varepsilon'_o$ and $\Delta\varepsilon'/\Delta\varepsilon''_o$, where $\Delta\varepsilon'$ and $\Delta\varepsilon''$ are the values of capacitance and dielectric loss at time t and $\Delta\varepsilon'$, $\Delta\varepsilon''_o$ are the maximum value obtained from the plateau of the individual master curves.

If the kinetics of the crystallization from the corresponding smectic phases are described by the above Avrami equation, the data for all the crystallization temperatures can be applied to the single equation [10]

$$x = 1 - \exp[1 - (t/t^*)^n] \tag{2}$$

where $t^* = b^{-1/n}$. Further, the characteristic time t^* can be experimentally determined, since at $t = t^*$, $x = 0.632$. Substituting the values of t^* and x in Eq. (1), constants b and n are obtained at a specified crystallization temperature. It is found from the experimental data that the constant n which manifests the dimensional geometry of the growing domains is almost unaltered while the magnitude of the constant b, which govern the nucleation mechanism, varies in the order of 10^{-1} to 10^{-6} for the compounds studied. The data of constants n and b experimentally obtained by DSC and dielectric studies (capacitance and dielectric loss) for various specified crystallization temperatures of 15O.8 and 15O.10 are tabulated in Table 2.

For a specified crystallization temperature, the values of constants n and b are found to be unaltered in both thermal and electrical studies implying that the same type of nucleation mechanism is taking place in both the nO·m compounds. The trend of the magnitude of the two constants n and b are found to be in agreement with the data reported for discotic [9] and smectic [4] mesophases. The variation of the magnitude of n in both the nO·m compounds is attributed to the sporadic nucleation and growth in two dimensions.

3.6. Influence of Tilted (Smectic F) Phase Variance on Crystallization Kinetics

The phase sequence in liquid crystal molecules has a pronounced influence on their crystallization kinetics. The kineto phase which occurs prior to the crystallization is solely responsible for many combinational factors of the crystallization mechanism.

In the present study of 15O.8 and 15O.10 compounds the kineto phase prior to crystallization is Smectic F. Our previous studies [4] on different nO·m compounds exhibiting various kineto phases concurred with data of the present investigations. Further in Smectic F, as expected, the rate of crystallization is rapid as it is close to crystalline phase. It is a known fact that crystallization kinetics will be fast for the crystallization temperatures (CT) near to crystal and slow when the CT is near the isotropic melt.

3.7. Influence of Alkyloxy Carbons

Both the 15O.8 and 15O.10 compounds have Smectic F as kineto phase, in which the molecules are tilted with respect to the director.

The data from Table 1 suggest the liquid crystalline phase thermal range is 41.6°C and 40.3°C for 15O.8 and 15O.10 compounds, respectively. Further the isotropic clearing point shifts to higher temperature with increase in carbon chain length, it is evident from Table 2, that the degree of variation of dimensionality parameter n infers a unique crystallization mechanism for these compounds. A possible explanation for crystallization dimensionality is a sporadic nucleation and growth involving a homogeneous process of continuous nucleation over a constant time [10]. Furthermore, the volume transformation calculated at individual crystallization time t^* is in accordance with equation (2) which strongly implies the completion of crystallization process.

3.8. Dielectric Studies

The dielectric studies enable to identify the phase transitions temperatures and the thermal range of individual phases. This study is a sophisticated tool to detect the second order transitions which cannot be identified by DSC studies.

To calculate the lead, capacitance, the liquid crystal cell is calibrated with a known (benzene) substance. Further, the empty liquid crystal cell is also calibrated against temperature in the range of 25°C to 150°C and with the frequency in the range of 100 Hz to 1 MHz, respectively. The compounds (15O.8 and 15O.10) are filled in a 4 micron spacer polyamide buffed cells (Instec Inc. USA) in its isotropic state under vacuum, the silver leads are drawn from to excite the cell with a frequency of 10 KHz and 100 KHz, respectively, obtained from an Agilent low frequency impedance analyzer (4192 A). This liquid crystal with compound is heated to its isotropic state and held for 10 minutes to attain thermal equilibrium. Further, it is cooled to crystal at a programmed scan rate of 0.1°C/min with an accuracy of ±0.01°C. This liquid crystal cell is placed in an Instec hot stage and is observed under crossed polars of a Nikon polarizing microscope. Simultaneous observation of the liquid crystal texture through polarizing microscope along with the dielectric data confirmed the formation and identification of the various smectic phases.

Compound 150.8 is chosen as a representative member of the present work, and the plot of capacitance with temperature at two frequencies *viz* 10 KHz and 100 KHz, respectively, is depicted in Fig. 4. Also variation of the capacitance with temperature for the empty cell is shown in Fig. 4 as solid line. The corresponding dielectric loss is illustrated in Fig. 5. The transition temperatures obtained from DSC, polarizing microscopic studies and dielectrics

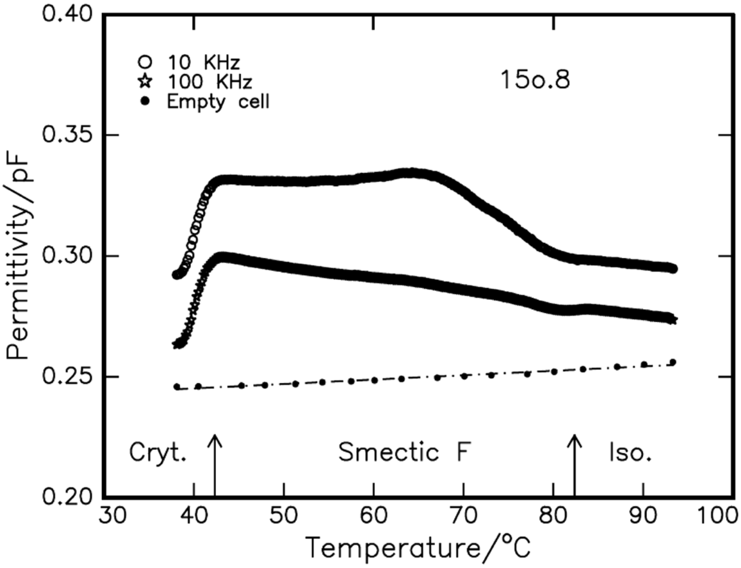

FIGURE 4 Temperature variation of capacitance at two frequencies (10 KHz and 100 KHz) identifying various liquid crystalline phases of 15O.8.

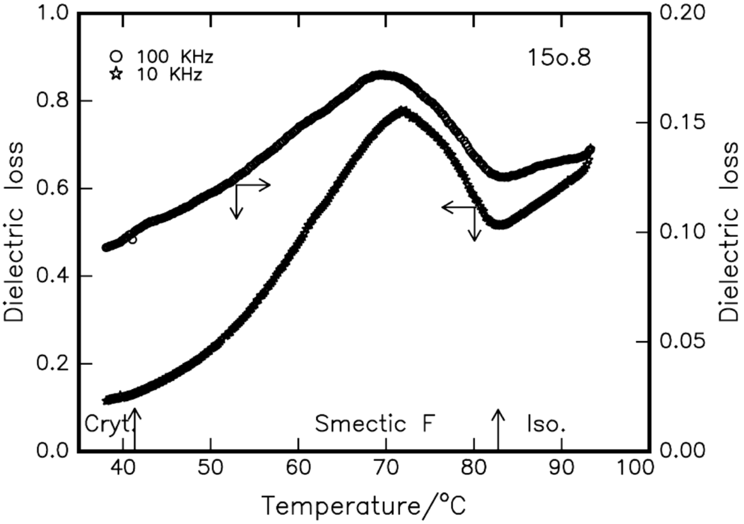

FIGURE 5 Temperature variation of dielectric loss at two frequencies (10 KHz and 100 KHz) identifying various liquid crystalline phases of 15O.8.

studies are compared in Table 1. The following points are noted from Figs. 4 and 5:

a) At isotropic to smectic F transition, a linear variation in both the profiles at 82.7°C and 82.7°C is observed, indicating the starting of smectic F phase. This transition occurred at 82.5°C from polarizing microscopic textural observation, which concurred with the dielectric studies.
b) The unaltered variation of the magnitudes of the capacitance and dielectric loss with lowering of temperature in the thermal range 82.7°C to 42.1°C is attributed to the stabilization of smectic F phase.
c) The transition from smectic F phase to crystal is marked by sudden decrement of capacitance and dielectric loss at 42.1°C and 41.5°C, respectively. The formation of crystal at 40.9°C is also evinced through polarizing microscopic textural studies, concurring with the transition temperatures obtained by dielectric studies.

It is prudent to mention that, in the present homologous series, the experimental results of 15o8 compound follows the same trend of 15O10 compound dielectric studies, as expected. These results are tabulated in Table 1. Furthermore, the transition temperatures obtained by various techniques, namely, dielectric studies, polarizing microscopic textural observations, and DSC thermograms are concurring with each other as can be seen from Table 1.

4. CONCLUSIONS

1. For the first time in the history of crystallization studies, crystallization kinetics data is experimentally elicited from a novel dielectric technique. Though the magnitude of the constants b obtained by both these techniques varies considerably, we claim that the trend of the crystallization kinetics result by this new technique is similar to that of the traditional thermal analysis.
2. In titled ordering (Smectic F) the formation of an ordered domain occurs which converts to a stable nucleus that initiates the aggregation of the surrounding molecules to form layered domains. The origin of this nucleus is critical since its formation proceeds until it reaches a sufficient size to initiate the crystallization process.
3. We propose that this process of crystallization is controlled by either the lamellar or interlayer distances in tilted (Smectic F) kineto phase. In such a process of seed nucleation, factors relating to the smectic layer plays an important role. A particular molecule

in the lower smectic layer first acquires the requisite energy to allow the formation of ordered domains, which in turn propagate crystallization to the adjacent smectic layers. These ordered domains will further proceed through the smectic layers by a process of successive addition of the molecules from neighboring layers leading to sporadic nucleation and growth in two dimensions. This process continues until the crystallization is completed.

4. The nucleation mechanism is found to be uniform in all the crystallization temperatures of both the nO·m compounds studied. This is manifested in Fig. 3, where log b is plotted against crystallization temperature. Further, from the dielectric studies the process of crystallization kinetics is observed to be identical.

ACKNOWLEDGMENTS

The authors thank the Management of Bannari Amman Institute of Technology for providing the laboratory and other infrastructural facilities. One of the authors (MLNMM), acknowledges the financial support provided by Department of Science and Technology, New Delhi, All India Council of Technical Education, New Delhi, and Defence Research Development Organization, New Delhi.

REFERENCES

[1] Demus, D. (1994). *Liquid Crystals: Phase Types Structures and Chemistry of Liquid Crystals*, Springer: New York.
[2] Avrami, M. (1939). *J. Chem. Phys.*, *7*, 1103.
[3] Avrami, M. (1940). *J. Chem. Phys.*, *8*, 212.
[4] Madhu Mohan, M. L. N., Arunachalam, B., & Aravind Sankar, C. R. (2008). *Met. Mat. Trans. A.*, *39*, 1192; Madhu Mohan, M. L. N. & Arunachalam, B. (2008). *Z. Naturforch*, *63a*, 435; Chitravel, T. Madhu Mohan, M. L. N., & Krishnakumar, V. Submitted to *Met. Mat. Trans. A.*; Kumar, P. A. Madhu Mohan, M. L. N., & Pisipati, V. G. K. M. (2000). *Liq. Cryst.*, *27*, 727.
[5] Madhu Mohan, M. L. N. (2008). Submitted to *Mat. Res. Bull.*
[6] Pisipati, V. G. K. M., Rao, N. V. S., Padmaja Rani, G., & Bhaskara Rao, P. (1991). *Mol. Cryst. Liq. Cryst. 210*, 165.
[7] Keller, P. & Scheurle, B. (1969). *Angew Chem. Int. Ed. Engl.*, *8*, 884.
[8] Gray, G. W. & Goodby, J. W. G. (1984). *Smectic Liquid Crystals—Textures and Structures*, Leonard Hill: London.
[9] Pisipati, V. G. K. M., George, A. K., Srinivasu, Ch., & Murty, P. N. (2002). *Z. Naturforsch*, *58a*, 103.
[10] Ziru, H., Yue, Z., & Caille, A. (1997). *Liq. Cryst.*, *23*, 317.